

A Deep-learning Model for Fast Prediction of Vacancy Formation in Diverse Materials

Kamal Choudhary^{*,†,‡} and Bobby G. Sumpter[¶]

[†]*Materials Science and Engineering Division, National Institute of Standards and Technology, Gaithersburg, 20899, MD, USA.*

[‡]*Theiss Research, La Jolla, 92037, CA, USA.*

[¶]*Center for Nanophase Materials Sciences, Oak Ridge National Laboratory, Oak Ridge, TN 37831, USA.*

E-mail: kamal.choudhary@nist.gov

Abstract

The presence of point defects such as vacancies plays an important role in material design. Here, we demonstrate that a graph neural network (GNN) model trained only on perfect materials can also be used to predict vacancy formation energies (E_{vac}) of defect structures without the need for additional training data. Such GNN-based predictions are considerably faster than density functional theory (DFT) calculations with reasonable accuracy and show the potential that GNNs are able to capture a functional form for energy predictions. To test this strategy, we developed a DFT dataset of 508 E_{vac} consisting of 3D elemental solids, alloys, oxides, nitrides, and 2D monolayer materials. We analyzed and discussed the applicability of such direct and fast predictions. We applied the model to predict 192494 E_{vac} for 55723 materials in the JARVIS-DFT database.

Defects play an important role in our pursuit to engineer performance of a material. Vacancies are a type of defects which are ubiquitous and their presence can significantly alter

catalytic, electronic, optoelectronic, electrochemical, diffusion, and neuromorphic properties.¹⁻¹⁰ Experimentally vacancy formation energies can be determined using positron annihilation experiments.¹¹ Theoretically, they can be computed using classical force-field (FF)^{12,13} and density functional theory (DFT)^{2,14-17} calculations. However, such computation can be very computationally expensive and non-generalizable for DFT and FF based calculations respectively.

Recently, machine learning techniques have been proposed as a faster method for predicting defect energetics, but so far they still require time-consuming defect data generation for model training and limit the applicability and generalizability of the defect energetic predictions.¹⁸⁻²³ Especially, graph neural network based deep-learning models²⁴⁻²⁷ have become very popular for predicting materials properties and have been used for several bulk property predictions and their applicability needs to be tested for defect property predictions. Two key ingredients needed for accomplishing this task are: 1) a pretrained deep-learning model that can directly predict the total energy of perfect and defect structures, 2) a test DFT dataset of vacancy formation energies on which the DL model could be applied.

In this work, we demonstrate that the atomistic line graph neural network (ALIGNN)²⁸ based total energy prediction model (trained on the JARVIS-DFT²⁹ OptB88vdW energy per atom data for perfect bulk materials²⁹) can be directly used to predict vacancy formation energy of an arbitrary material with reasonable accuracy without requiring additional training data. The performance in terms of mean absolute error for the energy per atom model was reported as 0.037 eV in ref.²⁸ Note that we do not train any machine learning/deep learning model in this work for defects and just used the model parameters for energy prediction that was developed and shared publicly in ref.²⁸

Developing a vacancy formation energy dataset can be extremely time-consuming and depends on several computational setup parameters such as supercell-size, choice of k-points, considering neutral vs. charged defects and selection of appropriate chemical potentials. For testing the strategy adopted in this work, we generated a DFT dataset of 508 entries with

charge neutral defects using a high-throughput approach. The dataset consists of elemental solids, oxide, alloy and 2D materials. In addition to predicting the vacancy formation energies, we analyze the trends, strengths and limitations of such predictions. Lastly, we used this strategy to develop a database of vacancy formation energies for all the materials in the JARVIS-DFT database. The deep-learning model, the DFT dataset and the workflow are made publicly available through the JARVIS (Joint Automated Repository for Various Integrated Simulations) infrastructure.²⁹

First, we discuss the generation of vacancy formation energy dataset that is used for testing the deep-learning model. We obtained stable elemental solids, binary alloys, oxides and 2D materials from the JARVIS-DFT dataset. We used at least 8 Å lattice parameter constraints in x,y,z directions to build the supercell. We removed an atom with a unique Wyckoff position to generate the vacancy structure using the JARVIS-Tools package (<https://github.com/usnistgov/jarvis>). The defect structures were then subjected to energy minimization using Optb88vdW functional³⁰ and projected augmented wave formalism³¹ in Vienna Ab initio Simulation Package (VASP) package.^{32,33} Please note commercial software is identified to specify procedures. Such identification does not imply recommendation by National Institute of Standards and Technology (NIST). We used the converged k-point and cut-off from the JARVIS-DFT dataset based on total energy convergence.³⁴ We used an energy convergence of 10^{-6} eV for energy convergence during the self-consistent cycle. Currently, we have 508 entries for the vacancies and the dataset is still growing.

For the deep-learning predictions, we used the recently developed atomistic line graph neural network (ALIGNN),²⁸ which is publicly available at <https://github.com/usnistgov/alignn>. ALIGNN has been used to train fast and accurate models for more than 65 properties of solids and molecules with high accuracy.^{25,28,35,36} In ALIGNN, a crystal structure is represented as a graph using atomic elements as nodes and atomic bonds as edges. Each node in the atomistic graph is assigned 9 input node features based on its atomic species: electronegativity, group number, covalent radius, valence electrons, first ionization energy,

electron affinity, block and atomic volume. The inter-atomic bond distances are used as edge features with radial basis function up to 8 Å cut-off and a 12-nearest-neighbor (N). This atomistic graph is then used for constructing the corresponding line graph using interatomic bond-distances as nodes and bond-angles as edge features. ALIGNN uses edge-gated graph convolution for updating nodes as well as edge features using a propagation function (f) for layer (l), atom features (h), and node (i), details of which can be found in Ref.:²⁸

$$h_i^{(l+1)} = f(h_i^l \{h_j^l\}_i) \quad (1)$$

Unlike many other conventional GNNs, ALIGNN uses bond-distances as well as bond-angles to distinguish atomic structures. The ALIGNN model is implemented in PyTorch³⁷ and deep graph library (DGL).³⁸ A model to predict energy per atom was developed in Ref²⁸ which will be used as an energy predictor for both perfect and defect structures in this work.

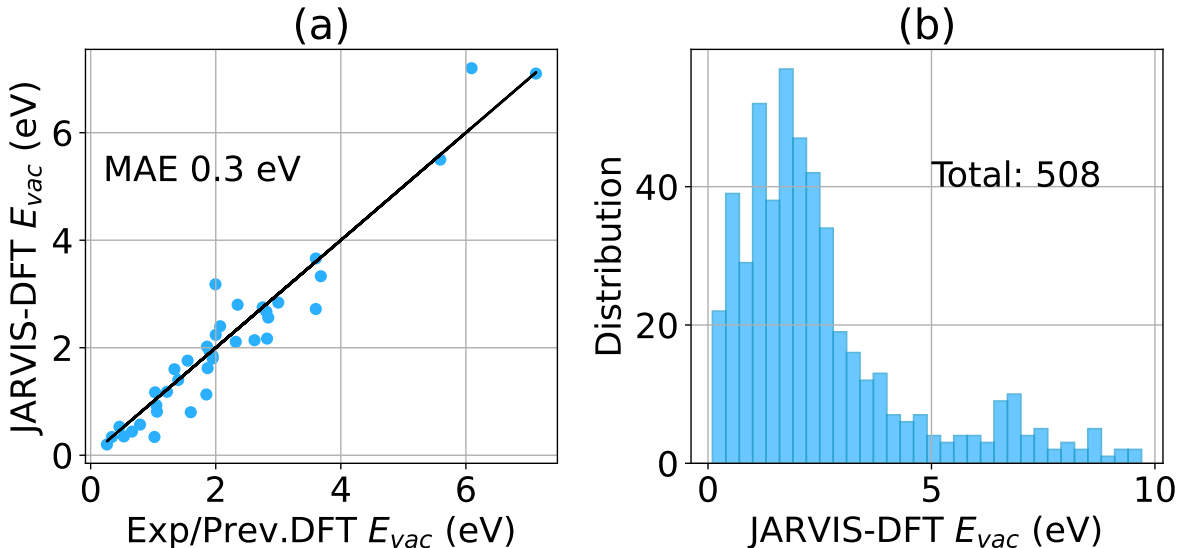


Figure 1: Analysis of vacancy formation energy dataset generated in this work. a) comparison of a subset of vacancy formation energy with respect to available experimental and previous DFT calculations from literature. Our dataset agrees very well with previously reported values. b) Data distribution of all the vacancy formation energy values. Most of the values are below 3 eV.

In Fig. 1 we analyzed the DFT database for vacancy formation energies developed in

this work. We used this dataset for testing purposes only. Although there have been several studies in generating vacancy formation energy dataset, a fully atomistic dataset consistent with bulk and vacancy energetics information is not available to our knowledge. Hence, we generated a DFT dataset for vacancies consisting of a wide variety of material classes such as elemental solids, 2D materials, oxides, and metallic alloys. We visualize the defect formation energies of materials in Fig. 1. As mentioned above, we only considered the charge neutral vacancies within a finite 8 Å cell size with OptB88vdW functional. The vacancy formation energy was calculated as

$$E_{vacancy} = E_{defect} - E_{perfect} + \mu \quad (2)$$

where, $E_{vacancy}$ is the vacancy formation energy, E_{defect} is the energy of the defect structure with an atom missing, $E_{perfect}$ is the energy of the perfect structure, μ is the chemical potential used as energy per atom of the most stable structure of an element. The chemical potentials used in this work are provided in the supplementary information.

Currently, the vacancy formation energy dataset consists of 508 entries. We compare a subset of this dataset with available data from previous experimental and DFT-studies^{14,39-43} in Fig. 1a. We find an excellent agreement between our dataset and that from literature with a mean absolute error (MAE) of 0.3 eV. In Fig. 1b, we show the histogram of all the vacancy formation energy data. We find that most of the vacancy formation energy data lie below 3 eV. Depending on the type of engineering applications, either a high or low E_{vac} could be desirable.

Next, we used ALIGNN based pretrained total energy per atom model trained on the JARVIS-DFT dataset for predicting defect energy and perfect energy required for vacancy formation energy following Eq. 2. This model was trained using bulk energies for 55723 solids.²⁸ The defect structures were generated by deleting an atom with a unique Wyckoff position without optimizing the atomic positions of other atoms in the defect structures. We used the same chemical potential for elements from the JARVIS-DFT as given in the supporting information. The comparison of ALIGNN based prediction with respect to DFT

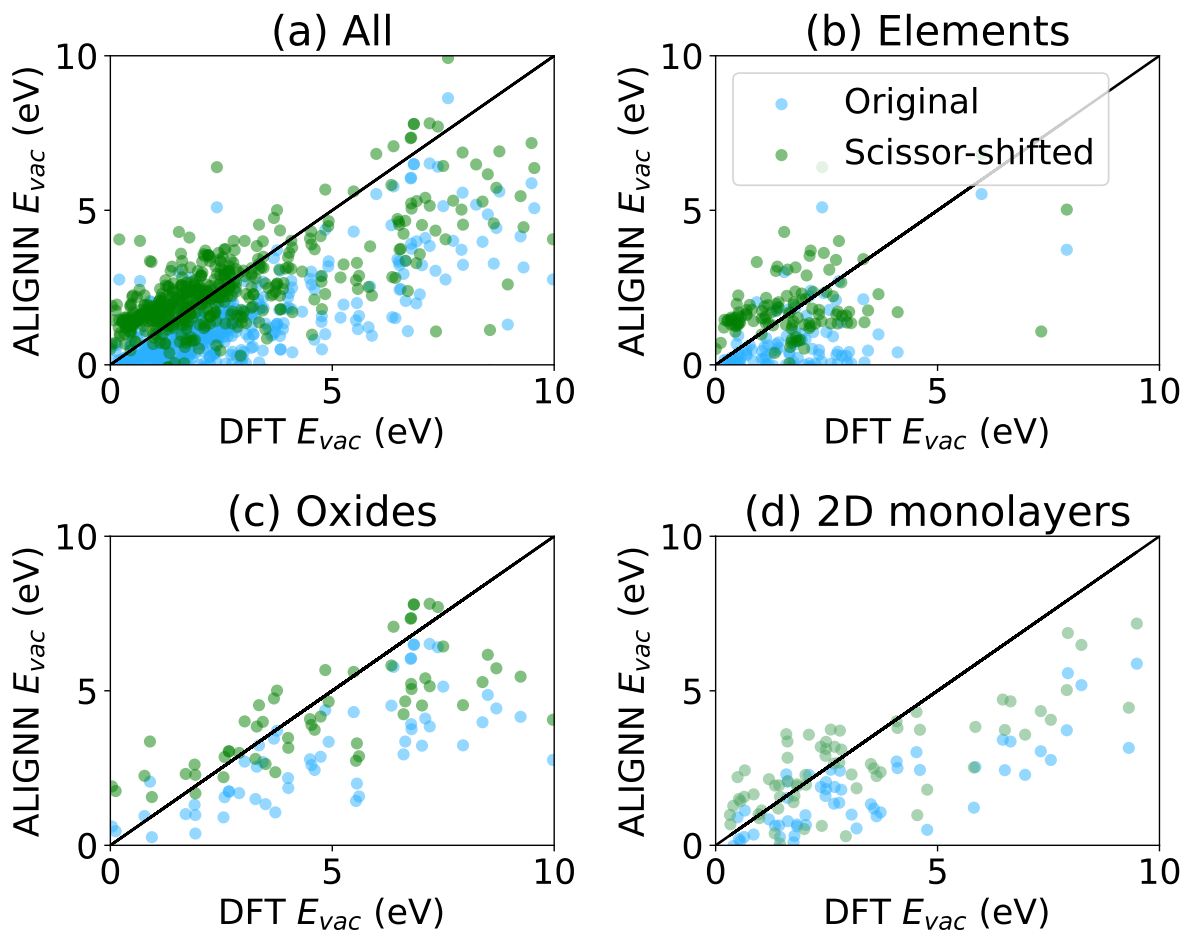


Figure 2: Comparison of DFT and ALIGNN based vacancy formation energy predictions with (Scissor-shift) and without (Original) correction. In Fig. a, we show the performance on the entire DFT dataset generated in this work. Fig.b,c,d show the comparisons for elemental solids, oxides and 2D monolayers respectively.

data is shown with blue dots in Fig. 2a. Interestingly, we observed that there is a noticeable correlation between the ALIGNN direct predictions and DFT data with a mean absolute error of 1.51 eV. However, we found that the ALIGNN based predictions were usually underestimated. To circumvent this issue, we applied a scissor shift by adding 1.3 eV to all the ALIGNN based predictions represented by green dots. Using such a shift, we were able to lower the MAE to 1.0 eV i.e., leading to an overall 33.8 % improvement. The value of 1.3 eV was chosen such that overall MAE is minimized. We noted that the previous reports on machine learning for vacancy formation energies resulted in mean absolute error values of

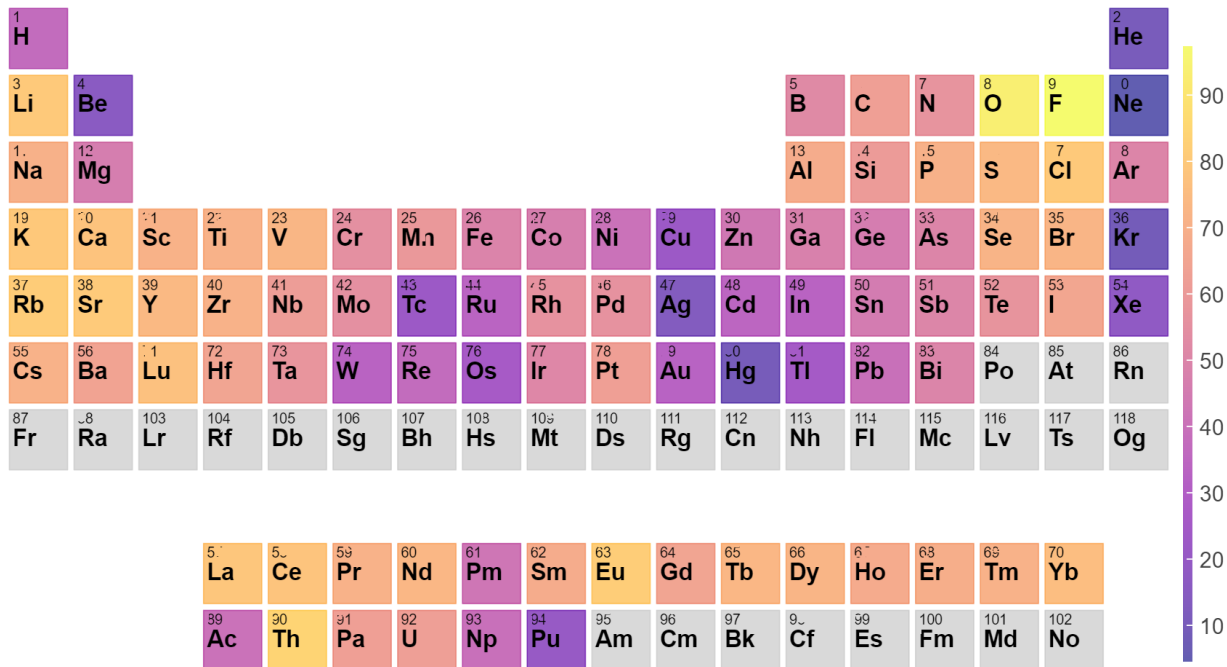


Figure 3: Periodic table trend of 192494 vacancy formation energies predicted from scissor-shifted ALIGNN based predictions. We visualize the probability that compounds with a vacancy of a given element have a vacancy formation energy more than 2 eV.

0.40 eV and 0.67 eV in ref.¹⁸ and ref.²¹ respectively. These models were trained on specific material classes such as GeTe system and 2D materials, while the approach used here acts as a generalized application of the model with MAE closer to specific case studies. Additionally, an MAE of 1.0 eV is arguably low considering the range of the vacancy formation energies can be up to 10 eV.

To further analyze the predictions for different types of materials, we compared the DFT and ALIGNN predictions for elemental solids, oxides and 2D monolayers in Fig. 2b, Fig. 2c and Fig. 2d respectively. Corresponding original ALIGNN prediction based MAE and that with scissor-shifted values are shown in Table 1. We found that the ALIGNN based models perform well for 2D monolayer and oxide materials compared to elemental solids and alloys. This behavior can be explained based on the fact that GNN architectures usually perform message passing locally and may work well for insulating materials with fewer bonds rather than for elemental solids and alloy systems which are usually metallic and have delocalized

Table 1: Analysis and comparison of ALIGNN based vacancy formation energy with respect to DFT dataset. The mean absolute errors (MAE) are calculated for all the values as well as elemental solid, oxide and 2D-monolayer subsets. The corresponding number of entries (Count) are also provided. As the ALIGNN based vacancy formation energies could be underestimated we apply scissor-shift and the improvement (% Δ) of predictions with (Scissor-shifted) and without scissor shift (Original) are shown.

Sets	Count	Original MAE	Scissor-shift MAE	% Δ
All	508	1.51	1.0	33.8
Elements	117	1.53	1.2	21.6
Oxides	57	2.3	1.4	30.4
2D-mono	68	1.9	1.2	36.8

electronic structures leading to a higher number of interatomic bonds.

To analyze the effect of training dataset size of energy per atom ALIGNN model on prediction of vacancy formation energies, we trained models for 20 %, 40 %, 60 %, 80 % and 100 % of total energy per atom training data for perfect materials resulting in mean absolute errors of 1.20 eV, 1.22 eV, 1.11 eV, 1.05 eV and 1.0 eV for vacancy formation dataset respectively. Therefore, one possible way to further improve the model would be to include more perfect structures that can have a varied number of bonds for various systems. As the JARVIS-DFT dataset for perfect structures is still growing, we believe the defect property prediction models should further improve in the future.

Now, we applied the above strategy to predict the vacancy formation energies of all the 55723 materials in the JARVIS-DFT leading to 192494 vacancy formation energies. In Fig. 3, we visualize the probability that compounds with the vacancy of a given element have vacancy formation energy of more than 2 eV as a threshold value. Interestingly, we found that C,N,O,F are some of the common elements with high vacancy formation energies. Furthermore, we plot the ALIGNN based vacancy formation energy dataset against OptB88vdW based formation energy available in the JARVIS-DFT database and color code with the corresponding OptB88vdW bandgaps in Fig. 4. We also provided the histogram distribution of the formation energy per atom and vacancy formation energy per atom. Interestingly, we found that high vacancy formation energies were favored by lower formation energies

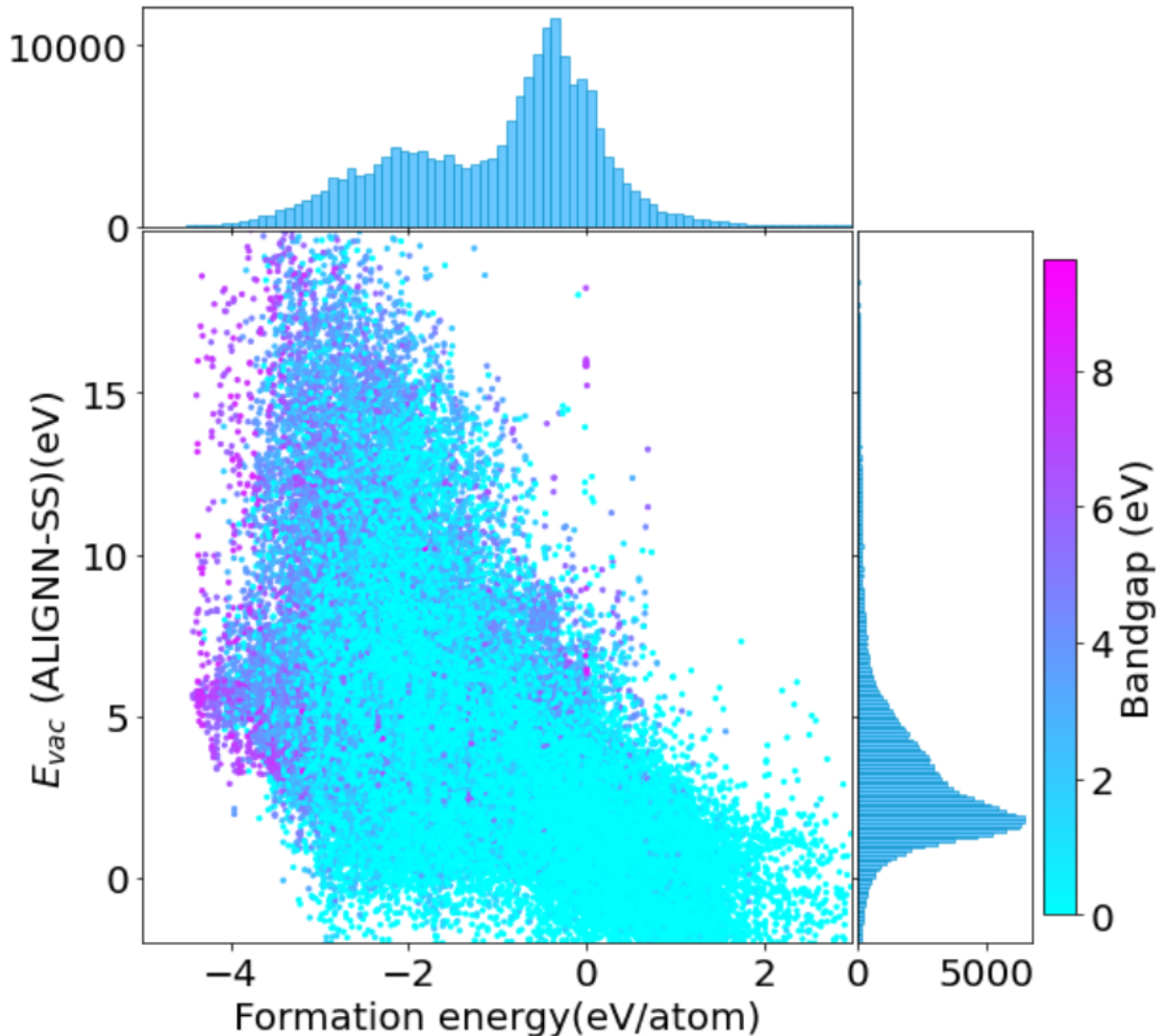


Figure 4: Figure shows ALIGNN vacancy formation energy with scissor-shift (SS) dataset (192494 entries) against OptB88vdW based formation energy available in the JARVIS-DFT database and color coded with corresponding OptB88vdW bandgaps.

per atom and high electronic bandgaps. The vacancy formation energy histogram showed a high peak around 2 eV which was similar to that observed in Fig. 1b. Such analysis helped us understand the entire dataset in a nutshell and can further help in understanding defect energetics for materials design for instance finding materials with high dopability, water splitting etc.

In summary, we have developed a diverse dataset of vacancy formation energies using density functional theory and demonstrate that the total energy per atom model using

ALIGNN can be directly used for predicting vacancy formation energies without the need for additional training data. The defect database can be highly useful for materials science community as there is a strong demand for a benchmark dataset. We have discussed the assumptions used in this work such as excluding charge defects and using finite cell sizes. Also, our work has shown how a state of the art model performs on unseen data without additional data. We have applied a heuristic scissor-shift of energy that further improves the accuracy. Using the current strategy, we have predicted vacancy formation energies of around 55723 compounds with 192494 entries leading to the largest dataset of defect properties, which could have been very expensive from DFT calculations. We provide data from this work as well as machine learning models to help accelerate the design of new materials. Our work has proven that GNN models can not only be useful for perfect materials but also defect systems.

Acknowledgement

K.C. thanks the National Institute of Standards and Technology for funding, computational, and data-management resources. Contributions from K.C. were supported by the financial assistance award 70NANB19H117 from the U.S. Department of Commerce, National Institute of Standards and Technology. DFT calculations were also conducted at the Center for Nanophase Materials Sciences, a US Department of Energy Office of Science User Facility.

Supporting Information Available

Experimental and previous DFT data for benchmarking, and chemical potential of elemental solids are provided in the supporting information.

References

- (1) Hinuma, Y.; Toyao, T.; Kamachi, T.; Maeno, Z.; Takakusagi, S.; Furukawa, S.; Takigawa, I.; Shimizu, K.-i. Density functional theory calculations of oxygen vacancy formation and subsequent molecular adsorption on oxide surfaces. *The Journal of Physical Chemistry C* **2018**, *122*, 29435–29444.
- (2) Emery, A. A.; Saal, J. E.; Kirklin, S.; Hegde, V. I.; Wolverton, C. High-throughput computational screening of perovskites for thermochemical water splitting applications. *Chemistry of Materials* **2016**, *28*, 5621–5634.
- (3) Watkins, M.; Pan, D.; Wang, E. G.; Michaelides, A.; VandeVondele, J.; Slater, B. Large variation of vacancy formation energies in the surface of crystalline ice. *Nature materials* **2011**, *10*, 794–798.
- (4) Emery, A. A.; Wolverton, C. High-throughput DFT calculations of formation energy,

- stability and oxygen vacancy formation energy of ABO₃ perovskites. *Scientific data* **2017**, *4*, 1–10.
- (5) Yu, X.; Zhan, Z.; Rong, J.; Liu, Z.; Li, L.; Liu, J. Vacancy formation energy and size effects. *Chemical Physics Letters* **2014**, *600*, 43–45.
- (6) Shang, S.-L.; Zhou, B.-C.; Wang, W. Y.; Ross, A. J.; Liu, X. L.; Hu, Y.-J.; Fang, H.-Z.; Wang, Y.; Liu, Z.-K. A comprehensive first-principles study of pure elements: Vacancy formation and migration energies and self-diffusion coefficients. *Acta Materialia* **2016**, *109*, 128–141.
- (7) Yan, X.; Zhao, Q.; Chen, A. P.; Zhao, J.; Zhou, Z.; Wang, J.; Wang, H.; Zhang, L.; Li, X.; Xiao, Z., et al. Vacancy-induced synaptic behavior in 2D WS₂ nanosheet-based memristor for low-power neuromorphic computing. *Small* **2019**, *15*, 1901423.
- (8) Parmar, N. S.; Boatner, L. A.; Lynn, K. G.; Choi, J.-W. Zn vacancy formation energy and diffusion coefficient of CVT ZnO crystals in the sub-surface micron region. *Scientific reports* **2018**, *8*, 1–8.
- (9) Ita, J.; Cohen, R. E. Effects of pressure on diffusion and vacancy formation in MgO from nonempirical free-energy integrations. *Physical Review Letters* **1997**, *79*, 3198.
- (10) Huh, W.; Lee, D.; Lee, C.-H. Memristors based on 2D materials as an artificial synapse for neuromorphic electronics. *Advanced Materials* **2020**, *32*, 2002092.
- (11) McKee, B.; Triftshäuser, W.; Stewart, A. Vacancy-formation energies in metals from positron annihilation. *Physical Review Letters* **1972**, *28*, 358.
- (12) Choudhary, K.; Biacchi, A. J.; Ghosh, S.; Hale, L.; Walker, A. R. H.; Tavazza, F. High-throughput assessment of vacancy formation and surface energies of materials using classical force-fields. *Journal of Physics: Condensed Matter* **2018**, *30*, 395901.

- (13) Huygh, S.; Bogaerts, A.; Van Duin, A. C.; Neyts, E. C. Development of a ReaxFF reactive force field for intrinsic point defects in titanium dioxide. *Computational materials science* **2014**, *95*, 579–591.
- (14) Medasani, B.; Haranczyk, M.; Canning, A.; Asta, M. Vacancy formation energies in metals: A comparison of MetaGGA with LDA and GGA exchange–correlation functionals. *Computational Materials Science* **2015**, *101*, 96–107.
- (15) Ding, H.; Medasani, B.; Chen, W.; Persson, K. A.; Haranczyk, M.; Asta, M. PyDII: a Python framework for computing equilibrium intrinsic point defect concentrations and extrinsic solute site preferences in intermetallic compounds. *Computer Physics Communications* **2015**, *193*, 118–123.
- (16) Goyal, A.; Gorai, P.; Anand, S.; Toberer, E. S.; Snyder, G. J.; Stevanovic, V. On the dopability of semiconductors and governing material properties. *Chemistry of Materials* **2020**, *32*, 4467–4480.
- (17) Goyal, A.; Gorai, P.; Peng, H.; Lany, S.; Stevanović, V. A computational framework for automation of point defect calculations. *Computational Materials Science* **2017**, *130*, 1–9.
- (18) Cheng, Y.; Zhu, L.; Wang, G.; Zhou, J.; Elliott, S. R.; Sun, Z. Vacancy formation energy and its connection with bonding environment in solid: A high-throughput calculation and machine learning study. *Computational Materials Science* **2020**, *183*, 109803.
- (19) Arrigoni, M.; Madsen, G. K. Evolutionary computing and machine learning for discovering of low-energy defect configurations. *npj Computational Materials* **2021**, *7*, 1–13.
- (20) Manzoor, A.; Arora, G.; Jerome, B.; Linton, N.; Norman, B.; Aidhy, D. S. Machine Learning Based Methodology to Predict Point Defect Energies in Multi-Principal Element Alloys. *Frontiers in Materials* **2021**, *8*, 129.

- (21) Frey, N. C.; Akinwande, D.; Jariwala, D.; Shenoy, V. B. Machine learning-enabled design of point defects in 2d materials for quantum and neuromorphic information processing. *ACS nano* **2020**, *14*, 13406–13417.
- (22) Mannodi-Kanakkithodi, A.; Xiang, X.; Jacoby, L.; Biegaj, R.; Dunham, S. T.; Gamelin, D. R.; Chan, M. K. Universal machine learning framework for defect predictions in zinc blende semiconductors. *Patterns* **2022**, *3*, 100450.
- (23) Sharma, V.; Kumar, P.; Dev, P.; Pilania, G. Machine learning substitutional defect formation energies in ABO₃ perovskites. *Journal of Applied Physics* **2020**, *128*, 034902.
- (24) Choudhary, K.; DeCost, B.; Chen, C.; Jain, A.; Tavazza, F.; Cohn, R.; Park, C. W.; Choudhary, A.; Agrawal, A.; Billinge, S. J., et al. Recent advances and applications of deep learning methods in materials science. *npj Computational Materials* **2022**, *8*, 1–26.
- (25) Choudhary, K.; Yildirim, T.; Siderius, D. W.; Kusne, A. G.; McDannald, A.; Ortiz-Montalvo, D. L. Graph neural network predictions of metal organic framework CO₂ adsorption properties. *Computational Materials Science* **2022**, *210*, 111388.
- (26) Fung, V.; Zhang, J.; Juarez, E.; Sumpter, B. G. Benchmarking graph neural networks for materials chemistry. *npj Computational Materials* **2021**, *7*, 1–8.
- (27) Fung, V.; Hu, G.; Ganesh, P.; Sumpter, B. G. Machine learned features from density of states for accurate adsorption energy prediction. *Nature communications* **2021**, *12*, 1–11.
- (28) Choudhary, K.; DeCost, B. Atomistic Line Graph Neural Network for improved materials property predictions. *npj Computational Materials* **2021**, *7*, 1–8.
- (29) Choudhary, K.; Garrity, K. F.; Reid, A. C.; DeCost, B.; Biacchi, A. J.; Hight Walker, A. R.; Trautt, Z.; Hattrick-Simpers, J.; Kusne, A. G.; Centrone, A.,

- et al. The joint automated repository for various integrated simulations (JARVIS) for data-driven materials design. *npj Computational Materials* **2020**, *6*, 1–13.
- (30) Klimeš, J.; Bowler, D. R.; Michaelides, A. Chemical accuracy for the van der Waals density functional. *Journal of Physics: Condensed Matter* **2009**, *22*, 022201.
- (31) Blöchl, P. E. Projector augmented-wave method. *Physical review B* **1994**, *50*, 17953.
- (32) Kresse, G.; Furthmüller, J. Efficient iterative schemes for ab initio total-energy calculations using a plane-wave basis set. *Physical review B* **1996**, *54*, 11169.
- (33) Kresse, G.; Furthmüller, J. Efficiency of ab-initio total energy calculations for metals and semiconductors using a plane-wave basis set. *Computational materials science* **1996**, *6*, 15–50.
- (34) Choudhary, K.; Tavazza, F. Convergence and machine learning predictions of Monkhorst-Pack k-points and plane-wave cut-off in high-throughput DFT calculations. *Computational materials science* **2019**, *161*, 300–308.
- (35) Choudhary, K.; Garrity, K. Designing High-Tc Superconductors with BCS-inspired Screening, Density Functional Theory and Deep-learning. *arXiv preprint arXiv:2205.00060* **2022**,
- (36) Kaundinya, P. R.; Choudhary, K.; Kalidindi, S. R. Prediction of the electron density of states for crystalline compounds with Atomistic Line Graph Neural Networks (ALIGNN). *arXiv preprint arXiv:2201.08348* **2022**,
- (37) Paszke, A.; Gross, S.; Massa, F.; Lerer, A.; Bradbury, J.; Chanan, G.; Killeen, T.; Lin, Z.; Gimelshein, N.; Antiga, L., et al. Pytorch: An imperative style, high-performance deep learning library. *Advances in neural information processing systems* **2019**, *32*.

- (38) Wang, M.; Zheng, D.; Ye, Z.; Gan, Q.; Li, M.; Song, X.; Zhou, J.; Ma, C.; Yu, L.; Gai, Y., et al. Deep graph library: A graph-centric, highly-performant package for graph neural networks. *arXiv preprint arXiv:1909.01315* **2019**,
- (39) Pham, H. H.; Wang, L.-W. Oxygen vacancy and hole conduction in amorphous TiO₂. *Physical Chemistry Chemical Physics* **2015**, *17*, 541–550.
- (40) Kumar, A.; Chernatynskiy, A.; Liang, T.; Choudhary, K.; Noordhoek, M. J.; Cheng, Y.-T.; Phillpot, S. R.; Sinnott, S. B. Charge optimized many-body (COMB) potential for dynamical simulation of Ni–Al phases. *Journal of Physics: Condensed Matter* **2015**, *27*, 336302.
- (41) Choudhary, K.; Liang, T.; Chernatynskiy, A.; Phillpot, S. R.; Sinnott, S. B. Charge optimized many-body (COMB) potential for Al₂O₃ materials, interfaces, and nanostructures. *Journal of Physics: Condensed Matter* **2015**, *27*, 305004.
- (42) Guo, Y.; Liu, D.; Robertson, J. Chalcogen vacancies in monolayer transition metal dichalcogenides and Fermi level pinning at contacts. *Applied Physics Letters* **2015**, *106*, 173106.
- (43) Wu, K.; Liu, T.; Sun, R.; Song, J.; Shi, C. First-principles calculations of oxygen vacancy in CaO crystal. *The European Physical Journal D* **2020**, *74*, 1–6.